Journal of Hazardous Materials 164 (2009) 172–181

Contents lists available at ScienceDirect

Journal of Hazardous Materials

journal homepage: www.elsevier.com/locate/jhazmat

Adsorption of methylene blue onto hazelnut shell: Kinetics, mechanism and activation parameters

Mehmet Doğan*, Harun Abak, Mahir Alkan

Balikesir University, Faculty of Science and Literature, Department of Chemistry, Cagis Campus, 10145 Balikesir, Turkey

ARTICLE INFO

Article history:
Received 13 May 2008
Received in revised form 29 July 2008
Accepted 30 July 2008
Available online 15 August 2008

Keywords:
Adsorption
Hazelnut shell
Methylene blue
Kinetic
Mechanism and activation parameters

ABSTRACT

The adsorption kinetics of methylene blue (MB) on the hazelnut shell with respect to the initial dye concentration, pH, ionic strength, particle size and temperature were investigated. The rate and the transport/kinetic processes of MB adsorption were described by applying the first-order Lagergren, the pseudo-second-order, mass transfer coefficient and the intraparticle diffusion models. Kinetic studies showed that the kinetic data were well described by the pseudo-second-order kinetic model. Significant increases in initial adsorption rate were observed with the increase in temperature followed by pH and initial MB concentration. The intraparticle diffusion was found to be the rate-limiting step in the adsorption process. Adsorption activation energy was calculated to be 45.6 kJ mol^{-1}. The values of activation parameters such as free energy (ΔG^*), enthalpy (ΔH^*) and entropy (ΔS^*) were also determined as 83.4 kJ mol^{-1}, 42.9 kJ mol^{-1} and −133.5 J mol^{-1} K^{-1}, respectively.

1. Introduction

The effluents of wastewater in some industries such as dyestuff, textiles, leather, paper, plastics, etc., contain various kinds of synthetic dyestuffs [1]. The effluents of these industries are highly colored and the discharge of these wastes into receiving waters causes severe damages to the environment [2]. The introduction of waste products into the environment is an important problem that has been highlighted by various environmentalist groups [3]. The dyestuffs have a complex chemical structure and are stable to light, heat and oxidation agents [4]. The source of such pollution lies in the rapid increase in the use of synthetic dyes. More than 10,000 chemically different dyes are being manufactured. The world dyestuff and dye intermediates production are estimated to be around 7×10^8 kg per annum [5,6]. Discharging of these dyes into water resources even in a small amount can affect the aquatic life and food web. Dyes can also cause allergic dermatitis and skin irritation. Some of them have been reported to be carcinogenic and mutagenic for aquatic organisms [3].

Although some existing technologies, such as chemical coagulation/flocculation, ozonation, cloud point extraction, oxidation processes, nanofiltration, chemical precipitation, ion-exchange, reverse osmosis and ultra filtration [3,7–9] may be efficient for the removal of the dyestuffs, these techniques are rather expensive. Application of biological processes to treat coloured wastewater is yet to be fully established. Among treatment technologies, adsorption is rapidly gaining prominence as a method of treating aqueous effluent. Activated carbon is the most effective and widely used adsorbent [10]. However, its high cost has prevented its application, at least in developing countries, so it is necessary to search for an alternative low-cost adsorbent which can be used as a substitute for activated carbon. A number of low cost adsorbents are reported in the literature. These include bagasse pith [11,12], maize cobs [10], sunflower [13], fly ash [14], peat [15], saw dust [16], marine algae [17], fungal biomass [18], wasted activated sludge [19], digested sludge [20], red mud [21], coir pith [22], Neem leaf [23], waste organic peel [24], tree fern [25]. However, sorption potential of most of these low cost sorbents is generally low.

Biosorption can be defined as sequestering of organic and inorganic species including metals, dyes and odor causing substances using live or dead biomass or their derivatives. Since the 1980s, biosorption has been continuously studied for the removal of heavy metals and other pollutants from wastewater, so it could be a promising alternative to replace or supplement present dye bearing wastewater treatment processes. Biosorption, if compared with other available technologies above, gives comparable performance at a very low cost. Apart from cost effectiveness and competitive performance, other advantages are possible regeneration at low cost, availability of known process equipment, sludge free operation and recovery of the sorbate [3]. The biosorption capacity of a biosorbent depends on several factors. It includes type of biosorbent (species, age), type of sorbate, and presence of other

* Corresponding author. Tel.: +90 266 612 1000; fax: +90 266 612 1215.
E-mail address: mdogan@balikesir.edu.tr (M. Doğan).

0304-3894/$ – see front matter © 2008 Elsevier B.V. All rights reserved.
doi:10.1016/j.jhazmat.2008.07.155

Nomenclature

C_t	dye concentration in solution at any time t (mol L^{-1})
C_0	initial dye concentration in aqueous solution (mol L^{-1})
E_a	activation energy (kJ mol^{-1})
ΔG^*	free energy of activation (kJ mol^{-1})
h_P	Planck's constant (J s)
ΔH^*	enhalpy of activation (kJ mol^{-1})
k_B	Boltzmann's constant (J K^{-1})
k_i	intraparticle diffusion rate constant (mol $min^{-1/2}$ g^{-1})
k_0	Arrhenius factor (g mol^{-1} min^{-1})
k_1	adsorption rate constant for pseudo-first-order kinetic equation (min^{-1})
k_2	adsorption rate constant for pseudo-second-order kinetic equation (g mol^{-1} min^{-1})
m	mass of adsorbent (g)
PS	particle size (μm)
q_e	equilibrium dye concentration on adsorbent (mol g^{-1})
q_t	the amount of dye adsorbed per unit mass of the adsorbent at time, t (mol g^{-1})
R^2	linear regression coefficient
R_g	gas constant (J K^{-1} mol^{-1})
ΔS^*	entropy of activation (J mol^{-1} K^{-1})
S_S	the surface area of adsorbent (m^2 g^{-1})
SS	stirring speed (rpm)
t	time (min)
$t_{1/2}$	the half-adsorption time of dye (min)
T	temperature (K)

Greek letter

β_L	mass transfer coefficient (m s^{-1})

competing ions and method of biomass preparation, along with several physico-chemical factors (temperature, pH, ionic concentration).

Hazelnut shells exist in large amounts in Turkey and Italy, as food industry waste. Its major use today is as combustible material owing the considerable calorific value. This material was considered in some works as source for activated carbon mostly utilized in removal of heavy metals. Hazelnut shells have the some polar functions such as alcoholic, carbonylic, carboxylic and phenolic groups, which are potentially involved in bonding with sorbed pollutants [26–28]. Ferrero [28] investigated the adsorption of some dyes such as methylene blue and acid blue 25 on hazelnut shell. But this paper does not include the effect of some parameters such as stirring speed, pH, temperature, ionic strength; the adsorption mechanism and also the activation parameters. The present work aims to study a convenient and economic method for methylene blue (MB) removal from water by adsorption on a low cost and an abundantly available adsorbent, to gain an understanding of the adsorption kinetics, to describe the rate and mechanism of adsorption, to determine the factors controlling the rate of adsorption and to calculate the activation energy of system. The effects of initial MB concentration, solution pH, ionic strength, particle size and temperature on MB adsorption rate have been evaluated. In this study, MB was selected as sorption of this dye has been reported by other researchers using different sorbents [22,29–35]. So, the sorption parameters obtained using the present biosorbent will be compared with the ones presented in the literature.

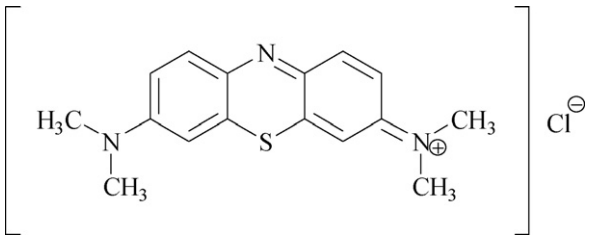

Fig. 1. The structure of MB.

2. Material and methods

2.1. Materials

Hazelnut shells were supplied from the Black Sea Region of Turkey. They were firstly dried, crushed in a ball mill and sieved to obtain a particle size between 0–75, 75–150 and 150–200 μm. MB was Merck product. The molecular structure of MB is reported in Fig. 1. Dye concentration determination was performed on a Perkin Elmer Lamda 25 UV–vis spectrophotometer at 663 nm. MB was chosen as the target compound because it has a net positive charge which would be favorably adsorbed by electrostatic force onto a negatively charged adsorbent surface. The aromatic moiety of MB contains nitrogen and sulfur atoms. In the aromatic unit, dimethylamino groups attach to it. The aromatic moiety is planar and the molecule is positively charged. The dimensions of MB molecule are16.9 Å for the length, 7.4 Å for the breadth, and 3.8 Å as thickness [36]. The specific surface area of the hazelnut shell was measured as 2.85 m^2 g^{-1} by Quantachrome Nova 2200e BET N2 instrument.

2.2. Adsorption kinetics

The experiments of adsorption kinetics were carried out to establish the effect of time on the adsorption process using a mechanice stirrer, and to identify the adsorption rate. Fig. 2 shows the schematic diagram of the batch adsorber. All of the dye solution was prepared with ultrapure water. In the adsorption experiments, 1 g of the hazelnut shell powders was mixed with 2 L solution at the desired MB concentrations, pHs, ionic strengths and temperatures. Agitation was made for 40 min, which is more than sufficient to reach equilibrium at a constant agitation speed of 200 rpm. The initial tested concentrations of MB solution were 1.0×10^{-4}, 2.0×10^{-4} and 3.0×10^{-4} mol L^{-1}. The effect of pH on the amount of color removal was analyzed in the pH range from 3 to 9. The pH was adjusted using 0.1N NaOH and 0.1N HCl solutions and measured by an Orion 920A pH-meter with a combined pH electrode. The pH-meter was standardized with NBS buffers before every measurement. The effect of ionic strength was investigated at 0.001–0.100 mol L^{-1} NaCl salt concentrations. The experiments were carried out at 30, 40, 50 and 60 °C in a constant temperature bath. 2 mL samples were drawn at suitable time intervals. The samples were then centrifuged for 15 min at 5000 rpm and the left out concentration in the supernatant solution were analyzed using a UV–vis spectrophotometer by monitoring the absorbance changes at a wavelength of maximum absorbance (663 nm). Preliminary experiments had shown that the effect of the separation time on the adsorbed amount of dye was negligible. Each experimental run continued until no significant change in the dye concentration was measured. Calibration curves were plotted between absorbance and concentration of the dye solution. The amount of MB adsorbed at time t (mol g^{-1}) onto the hazelnut shell (q_t, in mol g^{-1}) was calculated by a mass balance relationship,

$$q_t = (C_0 - C_t)\frac{V}{m} \quad (1)$$

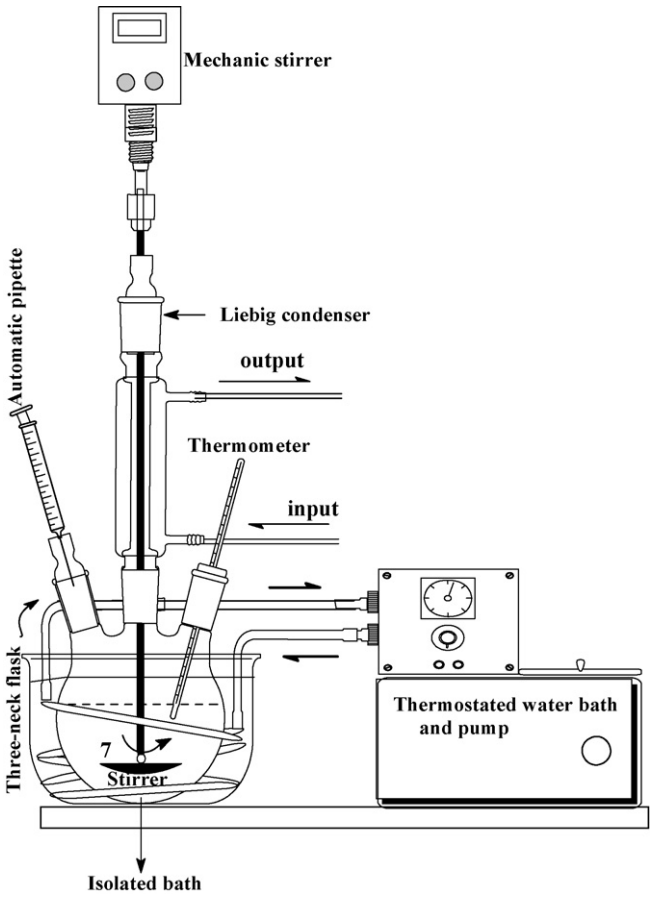

Fig. 2. Schema of the batch adsorber.

where C_0 is the initial MB concentration in solution (mol L^{-1}); C_t is the residual MB concentration in solution at time t (mol L^{-1}); V is the solution volume (L); m is the hazelnut shell mass (g) [37–39].

3. Results and discussion

3.1. Adsorption rate

To design effective and user-friendly adsorption model it was considered necessary to carry out adsorption with a kinetic viewpoint, and effects of contact time, stirring speed, initial MB concentration, initial solution pH, ionic strength, particle size and temperature on the uptake rate of the dye were monitored very carefully.

3.1.1. Effect of contact and equilibrium times

In order to determine the adsorption equilibrium time, the adsorption of the cationic MB dye onto hazelnut shell was studied as a function of contact time. The contact time between adsorbate and the adsorbent is of significant importance in the wastewater treatment by adsorption. The necessary contact time to reach the equilibrium depends on the initial dye concentration and the adsorption capacity increases with the initial dye concentration in all cases. A rapid uptake of adsorbates and establishment of equilibrium in short period stress the efficiency of that adsorbent for its use in wastewater treatment. Therefore, the contact time experiment for MB dye has been carried out with a constant initial dye concentration of 1×10^{-4} mol L^{-1}, particle size of 0–75 μm, solution pH (4.1–4.5), temperature 303 K and a constant stirrer speed

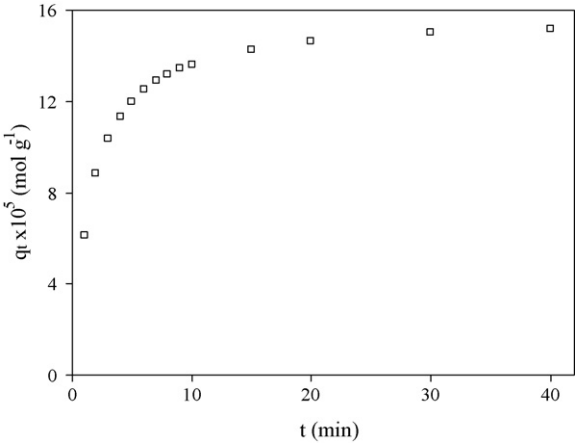

Fig. 3. The effect of contact time to the adsorption rate of MB on hazelnut shell (T: 30 °C, pH: 4.1–4.5, SS: 200 rpm, PS: 0–75 μm, C_0: 1×10^{-4} mol L^{-1}).

of 200 rpm. The amount of MB adsorbed on hazelnut shell is shown as a function of time in Fig. 3. Fig. 3 shows that the required contact time to reach the equilibrium of MB is 40 min. The contact time curve shows that the dye removal rate was rapid in the first 5 min due to surface adsorption. The curve of contact time is single, smooth and continuous leading to saturation due to intraparticle diffusion process. These curves indicate the possible monolayer coverage of dye on the surface of hazelnut shell [40,41]. Jain et al. [42] reported that a contact time of only about 25 min was required to attain the equilibrium adsorption of dyes to carbonaceous adsorbents. Again, we previously reported 30 min equilibrium contact time for removal of methyl violet, methylene blue and victoria blue by perlite at 30 °C [37–39].

3.1.2. Effect of stirring speed

The variation in the adsorption of MB as a function of stirring speed was studied using 1×10^{-4} mol L^{-1} initial dye concentration, 30 °C and solution pH. The effect of three stirring speeds was investigated: 200, 300 and 400 rpm. It appeared that stirring speed has no important influence on the adsorption of MB (figure not shown). Therefore, the stirring speed was taken as 200 rpm in further experiments.

3.1.3. Effect of initial MB concentration

The initial concentration provides an important driving force to overcome all mass transfer resistances of all molecules between the aqueous and solid phases [25,43]. The initial concentrations of MB solutions were changed and time intervals were assessed until no adsorption of adsorbate on hazelnut shell takes place. Fig. 4 shows the effects of contact time on the amount of MB adsorbed by hazelnut shell under different initial MB concentrations. As shown, the adsorption increases with increasing initial MB concentration. The removal of dye by adsorption on hazelnut shell was found to be rapid at the initial period of contact time and then to slow down with increasing in contact time. This was caused by attractive forces between the dye molecule and the adsorbent such as van der Waals forces and electrostatic attractions; fast diffusion onto the external surface was followed by fast pore diffusion into the intraparticle matrix, which contains the chromophere groups such as alcoholic, carbonylic and phenolic occurring of the adsorption, to attain rapid equilibrium. The increase in loading capacity of the adsorbent with relation to dye ions is probably due to a high driving force for mass transfer. In fact, the more concentrated the solution, the better the adsorption [44]. In other words, an increase in the surface loading led to a decrease in the adsorption rate. Generally, when adsorption

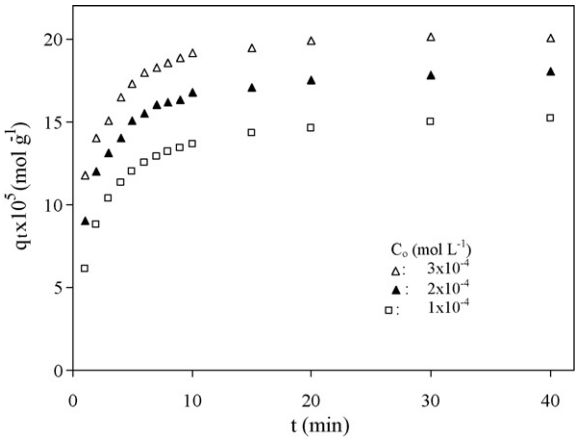

Fig. 4. The effect of initial dye concentration to the adsorption rate of MB on hazelnut shell (T: 30 °C, pH: 4.1–4.5, SS: 200 rpm, PS: 0–75 μm).

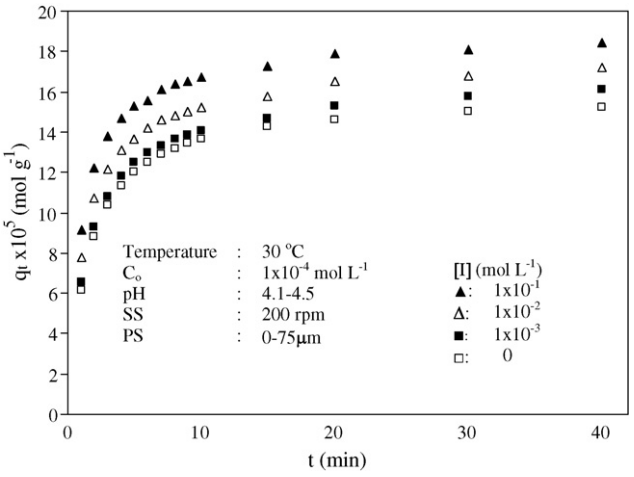

Fig. 6. The effect of ionic strength to the adsorption rate of MB on hazelnut shell.

involves a surface reaction process, the initial adsorption is rapid. Then, a slower adsorption would follow as the available adsorption sites gradually decrease [36].

3.1.4. Effect of initial solution pH

The pH is one of the most important factors controlling the adsorption of dye onto suspended particles. The pH of the solution affects the surface charge of the adsorbents as well as the degree of ionization of different pollutants. The hydrogen ion and hydroxyl ions are adsorbed quite strongly and therefore the adsorption of other ions is affected by the pH of the solution. Change of pH affects the adsorptive process through dissociation of functional groups on the adsorbent surface active sites. This subsequently leads to a shift in reaction kinetics and equilibrium characteristics of adsorption process. As the pH increases, it is usually expected that the cationic dye adsorption also increases due to increasing of the negative surface charge of adsorbents [38]. The effect of initial pH of the dye solution on the amount of dye adsorbed was studied by varying pHs under constant process parameters (Fig. 5). The removal of MB by hazelnut shell increased with pH change of dye solution from 3 to 9 at 30 °C. With increasing pH values the adsorption rate of MB on hazelnut shell tends to increase, which can be explained by the electrostatic interaction of cationic MB species with the negatively charged hazelnut shell surface. The electrostatic attraction force of the dye compound with the hazelnut shell surface is likely to be raised when the pH increases.

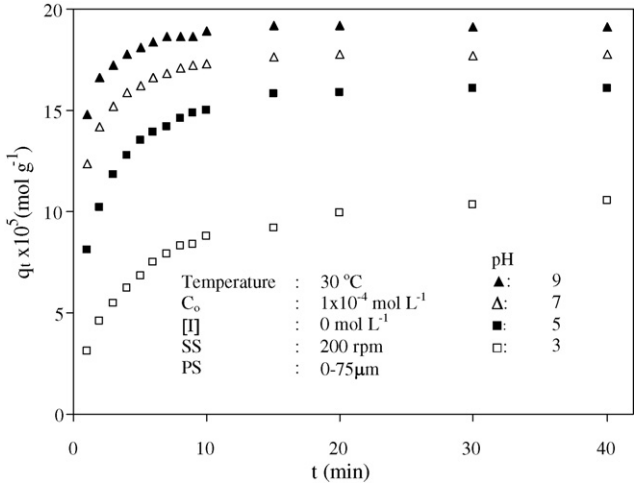

Fig. 5. The effect of pH to the adsorption rate of MB on hazelnut shell.

3.1.5. Effect of ionic strength

Extensive investigations carried out on adsorption of dyes revealed that the extent of dye uptake was strongly influenced by the concentration and nature of the electrolyte ionic species added to the dyebath [45]. The effect of inorganic salt (NaCl) on adsorption rate of MB on hazelnut shell is presented in Fig. 6. As seen in Fig. 6, the presence of inorganic salt has influenced the adsorption rate of MB. The dye adsorption lightly increases with the increasing NaCl concentration. This result is different from those reported by Janos et al. [46]. They tested the effect of inorganic salts (NaCl and $CaCl_2$) on some acid and basic dye adsorption and found that the dye adsorption was not affected. But in their investigation, the highest concentration of salts is only 2 mM, which is quite different from the present investigation. Our results show that higher concentration of salts promotes the adsorption of MB on hazelnut shell. The presence of NaCl in the solution may have two opposite effects. On the one hand, since the salt screens the electrostatic interaction of opposite changes of the surface and the dye molecule, the adsorbed amount should decrease with increase of NaCl concentration. On the other hand, the salt causes an increase in the degree of dissociation of the dye molecules by facilitating the protonation. The latter effect seems to be dominant on the adsorption capacity of the surface. For the adsorption of BBF by soils and malachite green by husk-based activated carbon, the adsorption was also found to increase with increasing ionic strength [47,48].

3.1.6. Effect of particle size

Adsorption rate of MB dye for three different particle sizes of hazelnut shell (0–75, 75–150 and 150–200 μm) was studied keeping the other parameters as constant. The results of variation of these particle sizes on dye adsorption rate are shown in Fig. 7. It can be observed that as the particle size decreases, the adsorption rate of the dye increases. This is due to larger surface area that is associated with smaller particles. For larger particles, the diffusion resistance to mass transport is higher and most of the internal surface of the particle may not be utilized for adsorption and consequently, the amount of dye adsorbed is small.

3.1.7. Effect of temperature

The effect of temperature on the adsorption rate of MB on hazelnut shell was investigated at 30, 40, 50 and 60 °C. The temperature has two major effects on the adsorption process. Increasing

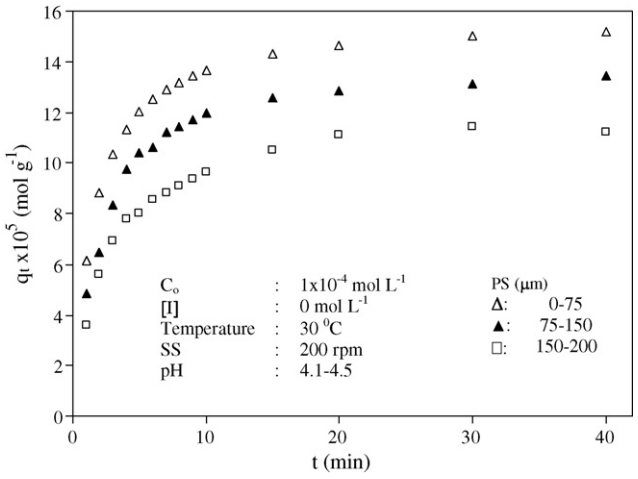

Fig. 7. The effect of particle size to the adsorption rate of MB on hazelnut shell.

the temperature is known to increase the rate of diffusion of the adsorbate molecules across the external boundary layer and in the internal pores of the adsorbent particle, owing to the decrease in the viscosity of the solution for highly concentrated suspensions. In addition, changing the temperature will change the equilibrium capacity of the adsorbent for a particular adsorbate [49]. Fig. 8 presents the contact time versus adsorbed amount, and indicates that with the increase in temperature the amount of adsorbed dye increases, indicating the process to be endothermic. This kind of temperature dependence of the adsorbed amount of MB may reflect the increase in the case with which the dye penetrates into the hazelnut shell because of its larger diffusion coefficient. In fact, a possible mechanism of interaction is the reaction between the chromophore groups such as alcoholic, carbonylic and phenolic of the hazelnut shell and the cationic group in the dye molecule; such a reaction could be favored at higher temperatures. Hydrogen bond can occur between —OH groups of hazelnut shell and nitrogen atom of dye; electrostatic attractive forces between cationic dye ions and the surface of hazelnut shell as depending on pH.

3.2. Adsorption kinetics

Adsorption is a physiochemical process that involves the mass transfer of a solute (adsorbate) from the fluid phase to the adsorbent surface. A study of kinetics of adsorption is desirable as it provides information about the mechanism of adsorption, which is important for efficiency of the process. The applicability of the pseudo-first-order and pseudo-second-order model was tested for the adsorption of MB onto hazelnut shell particles. The best-fit model was selected based on the linear regression correlation coefficient, R^2, values.

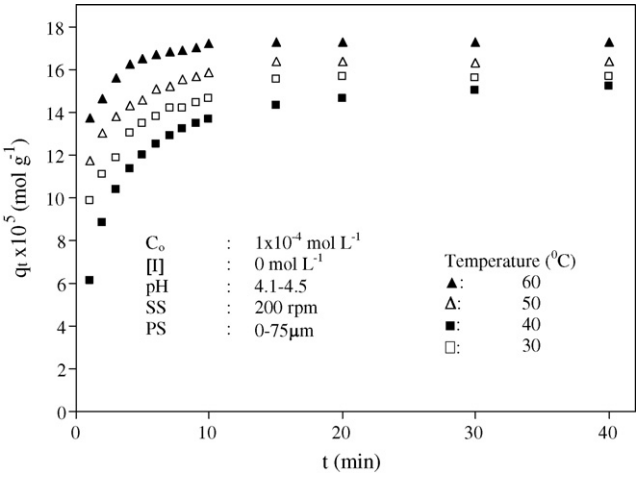

Fig. 8. The effect of temperature to the adsorption rate of MB on hazelnut shell.

3.2.1. The first-order kinetic model

The Lagergren rate equation is one of the most widely used adsorption rate equations for the adsorption of solute from a liquid solution. The pseudo-first-order kinetic model of Lagergren may be represented by [50]:

$$\frac{dq_t}{dt} = k_1(q_e - q_t) \tag{2}$$

Integrating this equation for the boundary conditions $t = 0$ to $t = t$ and $q = 0$ to $q = q_t$, gives:

$$\ln(q_e - q_t) = \ln q_e - k_1 t \tag{3}$$

where q_e and q_t are the amounts of MB adsorbed (mol g^{-1}) at equilibrium and at time t (min), respectively, and k_1 is the rate constant of pseudo-first-order adsorption (min^{-1}). The validity of the model can be checked by linearized plot of $\ln(q_e - q_t)$ versus t. The rate constant of pseudo-first-order adsorption is determined from the slope of the plot. The values of k_1 and q_e at different concentrations, initial solution pHs, ionic strength, particle sizes and temperatures are presented in Table 1.

3.2.2. The second-order kinetic model

The second-order kinetic model is expressed as

$$\frac{dq_t}{dt} = k_2(q_e - q_t)^2 \tag{4}$$

Rearranging the variables in Eq. (4) gives

$$\frac{dq_t}{(q_e - q_t)^2} = k_2\, dt \tag{5}$$

Taking into account, the boundary conditions $t = 0$ to $t = t$ and $q = 0$ to $q = q_t$, the integrated linear form of Eq. (5) can be rearranged to obtain Eq. (6):

$$\frac{t}{q_t} = \frac{1}{k_2 q_e^2} + \frac{t}{q_e} \tag{6}$$

The initial adsorption rate, h (mol g^{-1} min^{-1}) is expressed as

$$h = k_2 q_e^2 \tag{7}$$

where the initial adsorption rate (h), the equilibrium adsorption capacity (q_e), and the second-order constants k_2 (g mol^{-1} min^{-1}) can be determined experimentally from the slope and intercept of plot t/q_t versus t [51]. The k_2 and h values under different conditions were calculated and listed in Table 1.

As discussed above, the validity of the model of Lagergren and the pseudo-second-order kinetic model can be checked by each linearized plot. If the second-order kinetics is applicable, then the plot of t/q_t versus t should show a linear relationship. The linear plots of t/q_t versus t show good agreement between experimental ($q_{e(exp)}$) and calculated ($q_{e(cal)}$) values (Table 1). The correlation coefficients for the second-order kinetics model (R^2) are greater than 0.999, indicating the applicability of this kinetic equation and the second-order nature of the adsorption process of MB onto hazelnut shell. Similar phenomena have been observed for MB adsorption on coir pith carbon [52], cedar sawdust and crushed brick [53], perlite [38], sepiolite [54] and wheat shells [44].

Table 1
Kinetic data calculated for adsorption of MB on hazelnut shell

Parameters						Kinetic models						
						Pseudo-first-order model	Pseudo-second-order model					
T (°C)	$[C_0]$ (mol L^{-1}) × 10^4	pH	SS (rpm)	$[I]$ (mol L^{-1})	PS (μm)	R^2	$q_{e(cal)}$ (mol g^{-1}) × 10^5	$q_{e(exp)}$ (mol g^{-1}) × 10^5	k_2 (g mol^{-1} min^{-1}) × 10^3	R^2	$t_{1/2}$ (min)
30	1	4.1–4.5	200	0	0–75	0.9637	15.8	15.2	4.00	0.9999	1.58
40	1	4.1–4.5	200	0	0–75	0.8738	16.1	15.7	6.86	0.9997	0.91
50	1	4.1–4.5	200	0	0–75	0.9935	16.6	16.3	10.91	0.9997	0.55
60	1	4.1–4.5	200	0	0–75	0.8959	17.4	17.3	21.08	0.9998	0.27
30	1	3	200	0	0–75	0.9833	11.3	10.5	2.87	0.9999	3.07
30	1	5	200	0	0–75	0.9814	16.6	16.1	5.38	0.9998	1.12
30	1	7	200	0	0–75	0.9947	18.0	17.8	11.58	0.9999	0.48
30	1	9	200	0	0–75	0.9594	19.3	19.1	17.76	0.9999	0.29
30	2	4.1–4.5	200	0	0–75	0.9342	18.5	18.3	4.66	0.9999	1.16
30	3	4.1–4.5	200	0	0–75	0.9733	20.6	20.0	5.57	0.9997	0.87
30	1	4.1–4.5	200	0.001	0–75	0.9638	16.7	16.1	4.16	0.9998	1.44
30	1	4.1–4.5	200	0.010	0–75	0.9397	17.7	17.2	4.29	0.9998	1.31
30	1	4.1–4.5	200	0.100	0–75	0.9369	18.9	18.4	4.44	0.9999	1.19
30	1	4.1–4.5	200	0	75–150	0.9188	14.1	13.4	3.74	0.9998	1.90
30	1	4.1–4.5	200	0	150–200	0.9655	12.1	11.2	3.47	0.9991	2.38

The half-adsorption time, $t_{1/2}$, is defined as the time required for the adsorption to take up half as much hazelnut shell as its equilibrium value. This time is often used as a measure of the adsorption rate.

$$t_{1/2} = \frac{1}{k_2 q_e} \tag{8}$$

The values of $t_{1/2}$ determined for the tested parameters are given in Table 1. A further verification of the endothermic nature of the process was done by calculating the half-life of process at each temperature, which was found to decrease with increasing temperatures.

3.3. Adsorption mechanism

The prediction of the rate-limiting step is an important factor to be considered in sorption process. For solid–liquid sorption process, the solute transfer process was usually characterized by either external mass transfer (boundary layer diffusion) or intraparticle diffusion or both. The mechanism for the removal of MB by adsorption may be assumed to involve the following steps [55]:

1. Migration of dye from the bulk of the solution to the surface of adsorbent.
2. Diffusion of dye through the boundary layer to the surface of adsorbent.
3. Adsorption of dye at an active site on the surface of adsorbent.
4. Intraparticle diffusion of dye into the interior pore structure of adsorbent.

The boundary layer resistance will be affected by the rate of adsorption and increase in contact time, which will reduce the resistance and increase the mobility of dye during adsorption [44]. The uptake of MB at the active sites of hazelnut shell can mainly be governed by either liquid phase mass transfer rate or intraparticle mass transfer rate.

3.3.1. Mass transfer coefficient

Mass transfer coefficient, β_L (m s^{-1}) of MB at the hazelnut shell-solution interface, was determined by using Eq. (9) [56]:

$$\ln\left(\frac{C_t}{C_0} - \frac{1}{1+mK}\right) = \ln\left(\frac{mK}{1+mK}\right) - \left(\frac{1+mK}{mK}\right)\beta_L S_S t \tag{9}$$

where K is the Langmuir constant (L g^{-1}); m is the mass of adsorbent (g); and S_s is the surface area of adsorbent (m^2 g^{-1}). A linear graphical relation between $\ln[(C_t/C_0) - 1/(1+mK)]$ versus t was not obtained. This result indicates that the model mentioned above for the system is not validity. The values of regression coefficient calculated from equation mentioned above are given in Table 2.

3.3.2. Intraparticle diffusion

The adsorbate species are most probably transported from the bulk of the solution into the solid phase through an intraparticle diffusion process, which is often the rate-limiting step in many adsorption processes. The possibility of intraparticle diffusion was explored by using the intraparticle diffusion model [44]. An empirically found functional relationship, common to adsorption processes defines that the uptake varies almost proportionally with $t_{1/2}$, the Weber–Morris plot, rather than with the contact time t [57].

$$q_t = k_i \sqrt{t} + C \tag{10}$$

where k_i is the intraparticle diffusion rate constant (mol g^{-1} min$^{-1/2}$). According to Eq. (10), a plot of q_t versus $t_{1/2}$ should be a straight line with a slope k_i and intercept C when

Table 2
Adsorption mechanism of MB on hazelnut shell

Parameters						Adsorption mechanisms				
T (°C)	$[C_0]$ (mol L^{-1}) × 10^4	pH	SS (rpm)	$[I]$ (mol L^{-1})	PS (μm)	Mass transfer	Intraparticle diffusion			
						R^2	$k_{i1} \times 10^5$ (mol min$^{-1/2}$ g^{-1})	R^2	$k_{i2} \times 10^6$ (mol min$^{-1/2}$ g^{-1})	R^2
30	1	4.1–4.5	200	0	0–75	0.7047	4.35	0.9655	6.18	0.9224
40	1	4.1–4.5	200	0	0–75	0.6634	2.82	0.9883	4.43	0.7588
50	1	4.1–4.5	200	0	0–75	0.6634	2.32	0.9755	3.18	0.6866
60	1	4.1–4.5	200	0	0–75	0.5018	2.52	0.9924	1.65	0.816
30	1	3	200	0	0–75	0.7374	2.82	0.9952	6.31	0.9387
30	1	5	200	0	0–75	0.6650	4.06	0.9787	4.90	0.8963
30	1	7	200	0	0–75	0.6823	3.56	0.9866	3.29	0.6936
30	1	9	200	0	0–75	0.9537	2.92	0.9609	2.22	0.8442
30	2	4.1–4.5	200	0	0–75	0.5435	4.93	0.9577	6.72	0.8677
30	3	4.1–4.5	200	0	0–75	0.4932	4.46	0.9804	7.15	0.7397
30	1	4.1–4.5	200	0.001	0–75	0.8023	4.38	0.9621	7.59	0.9598
30	1	4.1–4.5	200	0.010	0–75	0.8628	4.73	0.9663	7.61	0.9525
30	1	4.1–4.5	200	0.100	0–75	0.9817	5.57	0.9732	7.39	0.9064
30	1	4.1–4.5	200	0	75–150	0.6477	3.99	0.9655	5.42	0.9877
30	1	4.1–4.5	200	0	150–200	0.6929	2.72	0.9371	5.01	0.8686

adsorption mechanism follows the intraparticle diffusion process. For intraparticle diffusion model, Ho [58] pointed out that it is essential for the q_t versus $t_{1/2}$ plots to go though the origin if the intraparticle diffusion is the sole rate-limiting step. The intraparticle diffusion plots are given in Figs. 9–13 for the effect of initial MB concentration, initial solution pH, ionic strength, particle size and temperatures on adsorption rate, respectively. The linearity of the plots demonstrated that intraparticle diffusion played a significant role in the uptake of MB by hazelnut shell powder. In the present study, any plot did not passed through the origin. This indicates that although intraparticle diffusion was involved in the adsorption process, it was not the sole rate-controlling step. This also confirms that adsorption of MB on the adsorbent was a multi-step process, involving adsorption on the external surface and diffusion into the interior [56]. From Figs. 9–13, at all conditions, the sorption process tends to be followed by two phases. It was found that an initial linear portion ended with a smooth curve followed by a second linear portion. The two phases in the intraparticle diffusion plot suggest that the sorption process proceeds by surface sorption and the intraparticle diffusion. The initial curved portion of the plot indicates boundary layer effect while the second linear portion is due to intraparticle or pore diffusion. The slope of second linear portion of the plot has been defined as the intraparticle diffusion parameter k_{i2} [59]. Table 2 shows the corresponding model fitting parameters, indicating the adsorption mechanism follows the intraparticle diffusion process. The intraparticle diffusion rate, k_{i2}, was in the range of 1.65×10^{-6} to 7.61×10^{-6} mol min$^{-1/2}$ g^{-1}. It was found that the values of k_{i2} increased with increasing initial

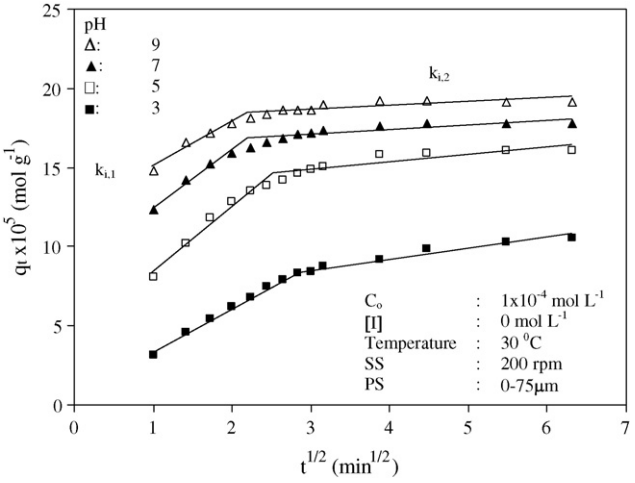

Fig. 10. Intraparticle diffusion plots for different initial solution pHs.

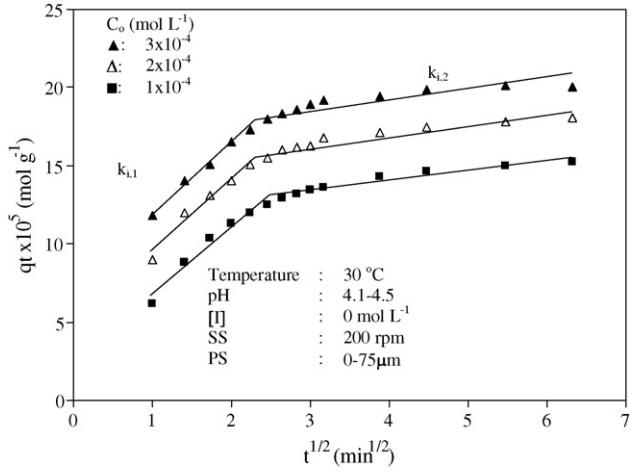

Fig. 9. Intraparticle diffusion plots for different initial MB concentrations.

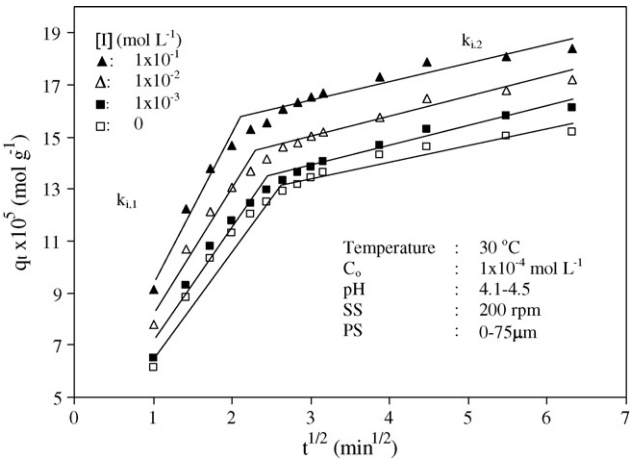

Fig. 11. Intraparticle diffusion plots for different ionic strengths.

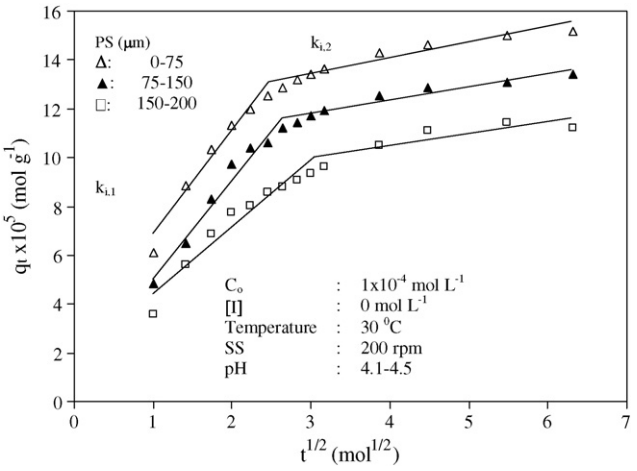

Fig. 12. Intraparticle diffusion plots for different particle sizes.

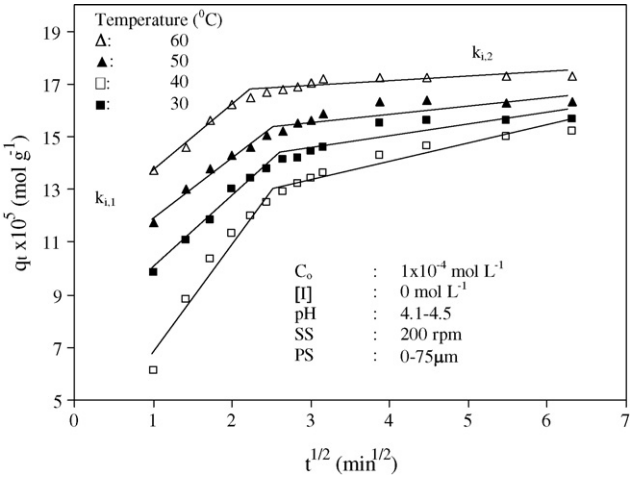

Fig. 13. Intraparticle diffusion plots for different temperatures.

MB concentration. The driving force of diffusion is very important for adsorption processes. Generally, the driving force changes with the adsorbate concentration in the bulk solution. The increase of adsorbate concentration results in an increase of the driving force, which will increase the diffusion rate of MB [36]. On the other hand, the intercept of the plot reflects the boundary layer effect. Larger the intercept, greater is the contribution of the surface sorption in the rate-limiting step. The calculated intraparticle diffusion coefficient k_{i2} value at different initial dye concentrations was shown in Table 2. Since the double nature of intraparticle diffusion plot confirms the presence of both surface adsorption and intraparticle diffusion [59].

Table 3 shows the adsorption orders and mechanisms of MB on various adsorbents from aqueous solutions. As seen in Table 3, similar results were found for coir pith carbon, cedar sawdust, crushed brick, perlite, sepiolite and wheat shells.

3.4. Activation parameters

The activation energy of dye adsorption onto the adsorbent can be calculated by Arrhenius relationship [60,61]

$$\ln k_2 = \ln k_0 - \frac{E_a}{R_g T} \quad (11)$$

where k_2 is the pseudo-second-order constant (g mol^{-1} min^{-1}), k_0 is the rate constant of adsorption (g mol^{-1} min^{-1}), E_a is activation energy of adsorption (J mol^{-1}), R_g is the gas constant (8.314 J mol^{-1} K^{-1}), T is the solution temperature (K). Plotting of $\ln k_2$ against the reciprocal temperature gives a reasonably straight line, the gradient of which is $-E_a/R_g$. From Eq. (11), the activation energy, E_a, is 45.6 kJ mol^{-1}. The magnitude of activation energy gives an idea about the type of adsorption which is mainly physical or chemical. Low activation energies (5–50 kJ mol^{-1}) are characteristics for physical adsorption, while higher activation energies (60–800 kJ mol^{-1}) suggest chemical adsorption [62]. This is because the temperature dependence of the pore diffusivity is relatively weak. Here, the diffusion process refers to the movement of the solute to an external surface of adsorbent and not diffusivity of material along micropore wall surfaces in a particle [60]. The result obtained for the adsorption of MB onto hazelnut shell indicates that the adsorption process is a physisorption (Fig. 14). Therefore, the affinity of MB for hazelnut shell may be ascribed to Van der Waals forces and electrostatic attractions between the dye and the surface of the particles. This low value of E_a generally indicates diffusion controlled process and higher values represent chemical reaction process. We can therefore conclude that the E_a value calculated from data suggest a diffusion-controlled process, which is a physical step in the adsorption process. This value is consistent with the values in the literature where the activation energy was found to be 43.0 kJ mol^{-1} for the adsorption of reactive red 189 on cross-linked chitosan beads [1], 5.6–49.1 kJ mol^{-1} for the adsorption of polychlorinated biphenyls on fly ash [63] and 33.96 kJ mol^{-1} for the adsorption of maxilon blue GRL on sepiolite [43].

To calculate the activation parameters such as enthalpy (ΔH^*), entropy (ΔS^*) and free energy (ΔG^*), the Eyring equation was applied [64],

$$\ln\left(\frac{k_2}{T}\right) = \ln\left(\frac{k_B}{h_P}\right) + \frac{\Delta S^*}{R_g} - \frac{\Delta H^*}{R_g T} \quad (12)$$

Table 3
Adsorption order and mechanism of MB dye on various adsorbents

Adsorbents	Adsorption order	Adsorption mechanism	References
Modified diatomite	Pseudo-second-order	Intraparticle diffusion	[60]
Chitosan	Lagergren-first-order	Intraparticle diffusion	[31]
Bio-sludge ash	Modified Freundlich equation	Intraparticle diffusion	[36]
Coir pith carbon	Pseudo-second-order	Intraparticle diffusion	[52]
Neem leaf powder	Pseudo-first-order	Surface adsorption and pore diffusion	[56]
Cedar sawdust	Pseudo-second-order	Film- and particle diffusion	[53]
Crushed brick	Pseudo-second-order	Film- and particle diffusion	[53]
Wheat shells	Pseudo-second-order	–	[44]
Activated carbon	Pseudo-first-order	Intraparticle diffusion	[29]
Perlite	Pseudo-second-order	Intraparticle diffusion	[38]
Sepiolite	Pseudo-second-order	Intraparticle diffusion	[54]
Hazelnut shell	Pseudo-second-order	Intraparticle diffusion	In this study

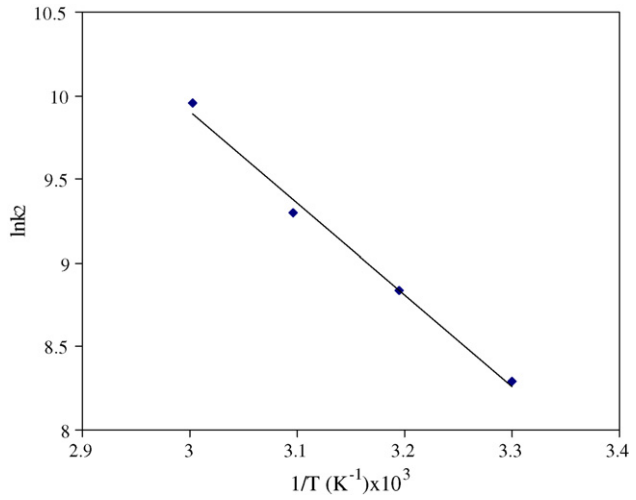

Fig. 14. Arrhenius plot for the adsorption of MB on hazelnut shell.

where k_B is the Boltzmann constant (1.3807×10^{-23} J K^{-1}), h_P is the Planck constant (6.6261×10^{-34} J s), k_2 is the pseudo-second-order constant (k_2). Fig. 15 has shown the plot of $\ln(k_2/T)$ against $1/T$. Gibbs energy of activation may be written in terms of entropy and enthalpy of activation:

$$\Delta G^* = \Delta H^* - T\Delta S^* \quad (13)$$

The result obtained for the change of activation Gibbs energy is +83.4 kJ mol^{-1} at 30 °C. The positive ΔG^* value suggests that adsorption reactions require energy to convert reactants into products. The ΔG^* value determines the rate of the reaction, rate increases as ΔG^* decreases, and hence the energy requirement is fulfilled, the reaction proceeds. The positive value of ΔH^* (42.9 kJ mol^{-1}) confirms the endothermic process, meaning the reaction consume energy. The negative value of ΔS^* (-133.5 J K^{-1} mol^{-1}) indicates that the adsorption leads to order through the formation of activated complex suggesting that methylene blue adsorption on hazelnut shell surface is an associated mechanism. Also the negative value of ΔS^* normally reflects that no significant change occurs in the internal structure of the adsorbent during the adsorption process [65].

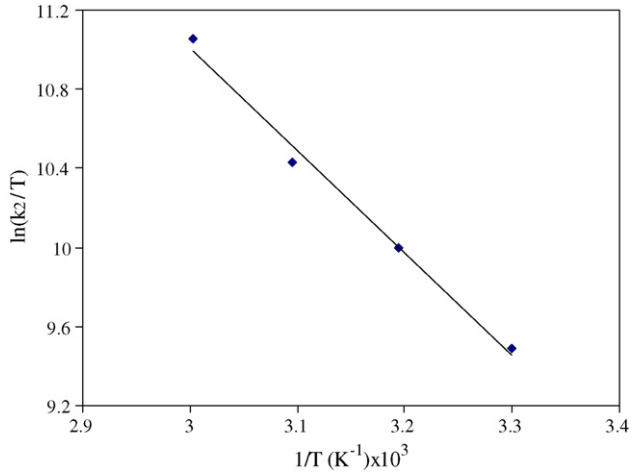

Fig. 15. Plot of $\ln(k_2/T)$ versus $1/T$ for adsorption of MB on hazelnut shell.

4. Conclusions

Adsorption of cationic MB dye on hazelnut shell can be considered as a simple, fast and economic method for its removal from water and wastewater. A very good agreement with experimental data obtained indicates that a pseudo-second-order kinetic model is favorable for the MB adsorption on hazelnut shell. The correlation coefficients were between 0.9991 and 0.9999. In addition, it was clear that the MB adsorption onto hazelnut shell was intraparticle diffusion controlled. Significant increasing in initial adsorption rate observed with the increase in temperature, followed by pH and initial MB concentration. Results show that dye adsorption onto hazelnut shell particles is a fast process. It reaches equilibrium in 40 min. The changing solution temperature of dye adsorption has increased the rate of diffusion of dye molecules across the external boundary layer and in the internal pores of the hazelnut shell particle. The activation parameters of the adsorption process helped in predication of how the adsorption of dye molecules might vary with temperature changes. The activation energy, E_a, was 45.6 kJ mol^{-1}. The activation enthalpy, entropy and free energy changes for adsorption are estimated to be 42.9 kJ mol^{-1}, -133.5 J mol^{-1} K^{-1} and 83.4 kJ mol^{-1}, respectively. The positive value of ΔH^* (42.9 kJ mol^{-1}) confirms the endothermic process, meaning the reaction consume energy. The negative value of ΔS^* (-133.5 J K^{-1} mol^{-1}) indicates that the adsorption leads to order through the formation of activated complex suggesting that methylene blue adsorption on hazelnut shell surface is an associated mechanism. The optimum conditions for adsorption process were determined as high concentration, ionic strength and pH; and low particle size and temperature.

References

[1] M.S. Chiou, H.Y. Li, Adsorption behaviour of reactive dye in aqueous solution on chemical cross-linked chitosan beads, Chemosphere 50 (2003) 1095–1105.
[2] Z. Aksu, S. Tezer, Equilibrium and kinetic modelling of biosorption of remazol black B by Rhizopus arrhizus in a batch system: effect of temperature, Process Biochem. 36 (2001) 431–439.
[3] E. Lorenc-Grabowska, G. Gryglewicz, Adsorption characteristics of Congo Red on coal-based mesoporous activated carbon, Dyes Pigments 74 (2007) 34–40.
[4] I.K. Kapdan, F. Kargi, Simultaneous biodegradation and adsorption of textile dyestuff in an activated sludge unit, Process Biochem. 37 (2002) 973–981.
[5] Y. Fu, T. Viraraghavan, Fungal decolorization of dye wastewaters: a review, Bioresour. Technol. 79 (2001) 251–262.
[6] Y.C. Toh, J.J.L. Yen, P.O. Jeffrey, Y.P. Ting, Decolourisation of azo dyes by white-rot fungi (WRF) isolated in Singapore, Enzyme Microb. Technol. 35 (5) (2003) 569–575.
[7] P.K. Malik, S.K. Saha, Oxidation of direct dyes with hydrogen peroxide using ferrous ion as catalyst, Sep. Purif. Technol. 31 (2003) 241–250.
[8] P.K. Malik, S.K. Sanyal, Kinetics of decolourisation of azo dyes in wastewater by UV/H_2O_2 process, Sep. Purif. Technol. 36 (2004) 167–175.
[9] I.M. Banat, P. Nigam, D. Singh, R. Marchant, Microbial decolorization of textile-dye-containing effluents: a review, Bioresour. Technol. 58 (1996) 217–227.
[10] M.S. El-Geundi, Colour removal from textile effluents by adsorption techniques, Water Res. 25 (1991) 271–273.
[11] M.M. Nassar, M.S. El-Geundi, Comparative cost of colour removal from textile effluents using natural adsorbents, J. Chem. Technol. Biotechnol. 50 (2) (1991) 257–264.
[12] G. McKay, M. El-Geundi, M.M. Nassar, External mass transport processes during the adsorption of dyes onto bagasse pith, Water Res. 22 (12) (1988) 1527–1533.
[13] G. Sun, X. Xu, Sunflower stalks as adsorbents for color removal from textile wastewater, Ind. Eng. Chem. Res. 36 (3) (1997) 808–812.
[14] V.K. Gupta, D. Mohan, S. Sharma, M. Sharma, Removal of basic dye (Rhodamine B and Methylene blue) from aqueous solutions using bagasse fly ash, Sep. Sci. Technol. 35 (2000) 2097–2113.
[15] K.R. Ramakrishna, T. Viraraghavan, Dye removal using peat, Am. Dyestuff Rep. 85 (10) (1996) 28–34.
[16] T.H. El-Nabarwy, S.A. Khedr, Removal of pollutants from water using untreated and treated sawdust and water hyacinth, Adsorp. Sci. Technol. 18 (4) (2000) 385–398.

[17] X.K. Zhao, G.P. Yang, X.C. Gao, Studies on the sorption behaviors of nitrobenzene on marine sediments, Chemosphere 52 (2003) 917–925.
[18] M. Basibuyuk, C.F. Forster, An examination of the adsorption characteristics of a basic dye (Maxilon Red BL-N) on to live activated sludge system, Process Biochem. 38 (2003) 1311–1316.
[19] G. Annadurai, R.S. Juang, P.S. Yen, D.J. Lee, Use of thermally treated waste biological sludge as dye absorbent, Adv. Environ. Res. 7 (2003) 739–744.
[20] C.H. Weng, E.E. Chang, P.C. Chiang, Characteristics of new coccine dye adsorption onto digested sludge particulates, Water Sci. Technol. 44 (2001) 279–284.
[21] C. Namasivayam, D.J.S.E. Arasi, Removal of Congo red from wastewater by adsorption onto red mud, Chemosphere 34 (1997) 401–471.
[22] C. Namasivayam, K.M. Dinesh, K. Selvi, A.R. Begum, T. Vanathi, R.T. Yamuna, Waste coir pith—a potential biomass for the treatment of dyeing wastewaters, Biomass Bioenergy 21 (2001) 477–483.
[23] K.G. Bhattacharyya, A. Sarma, Adsorption characteristics of the dye, Brilliant green, on Neem leaf powder, Dyes Pigments 57 (2003) 211–222.
[24] C. Namasivayam, N. Muniasamy, K. Gayathri, M. Rani, K. Ranganathan, Removal of dyes from aqueous solutions by cellulosic waste orange peel, Bioresour. Technol. 57 (1996) 37–43.
[25] Y.S. Ho, T.H. Chiang, Y.M. Hsueh, Removal of basic dye from aqueous solutions using tree fern as a biosorbent, Process Biochem. 40 (2005) 119–124.
[26] W. Heschel, E. Klose, On the suitability of agricultural by-products for the manufacture of granular activated carbon, Fuel 74 (1995) 1786–1791.
[27] A. Demirbas, Properties of charcoal derived from hazelnut shell and the production of briquettes using pyrolytic oil, Energy 24 (1999) 141–150.
[28] F. Ferrero, Dye removal by low cost adsorbents: hazelnut shells in comparison with wood sawdust, J. Hazard. Mater. 142 (2007) 144–152.
[29] N. Kannan, M.M. Sundaram, Kinetics and mechanism of removal of methylene blue by adsorption on various carbons—a comparative study, Dyes Pigments 51 (2001) 25–40.
[30] S.G. Miguel, G.D. Fowler, C.J. Sollars, Adsorption of organic compounds from solution by activated carbons produced from waste tyre rubber, Sep. Sci. Technol. 37 (3) (2002) 663–676.
[31] G. Annadurai, R.S. Juang, D.J. Lee, Use of cellulose-based wastes for adsorption of dyes from aqueous solutions, J. Hazard. Mater. B92 (2002) 263–274.
[32] Y. Fu, T. Viraraghavan, Dye biosorption sites in *Aspergillus niger*, Bioresour. Technol. 82 (2002) 139–145.
[33] F. Rozada, L.F. Calvo, A.I. Garcia, J. Martin-Villacorta, M. Otero, Dye adsorption by sewage sludge-based activated carbons in batch and fixed-bed systems, Bioresour. Technol. 87 (2003) 221–230.
[34] A.S. Reyad, F.T. Maha, Experimental study and modeling of basic dye sorption by diatomaceous clay, Appl. Clay Sci. 24 (2003) 111–120.
[35] J. Pavel, B. Hana, R. Milena, Sorption of dyes from aqueous solutions onto fly ash, Water Res. 37 (2003) 4938–4944.
[36] C.-H. Weng, Y.-F. Pan, Adsorption characteristics of methylene blue from aqueous solution by sludge ash, Colloids Surf. A: Physicochem. Eng. Aspects 274 (2006) 154–162.
[37] M. Doğan, M. Alkan, Adsorption kinetics of methyl violet onto perlite, Chemosphere 50 (2003) 517–528.
[38] M. Doğan, M. Alkan, A. Türkyılmaz, Y. Özdemir, Kinetics and mechanism of removal of methylene blue by adsorption onto perlite, J. Hazard. Mater. B109 (2004) 141–148.
[39] M. Alkan, M. Doğan, Adsorption kinetics of ÿklanÿia blue onto perlite, Fresenius Environ Bull. 12 (5) (2003) 418–425.
[40] M. Dogan, M. Alkan, Removal of methyl violet from aqueous solutions by perlite, J. Colloid Interface Sci. 267 (2003) 32–41.
[41] P.K. Malik, Use of activated carbons prepared from sawdust and ricehusk for adsorption of acid dyes: a case study of acid yellow 36, Dyes Pigments 56 (2003) 239–249.
[42] A.K. Jain, V.K. Gupta, A. Bhatnagar, Suhas, A comparative study of adsorbents prepared from industrial wastes for removal of dyes, Sep. Sci. Technol. 38 (2003) 463–481.
[43] M. Doğan, M. Alkan, Ö. Demirbas, Y. Ozdemir, C. Ozmetin, Adsorption kinetics of maxilon blue GRL onto sepiolite from aqueous solutions, Chem. Eng. J. 124 (2006) 89–101.
[44] Y. Bulut, H. Aydın, A kinetics and thermodynamics study of methylene blue adsorption on wheat shells, Desalination 194 (2006) 259–267.
[45] Y. Özdemir, M. Doğan, M. Alkan, Adsorption of cationic dyes from aqueous solutions by sepiolite, Microporous Mesoporous Mater. 96 (1–3) (2006) 419–427.
[46] P. Janos, H. Buchtova, M. Ryznarova, Sorption of dyes from aqueous solutions onto fly ash, Water Res. 37 (2003) 4938–4944.
[47] J. German-Heins, M. Flury, Sorption of brilliant blue FCF in soils as affected by pH and ionic strength, Geoderma 97 (2000) 87–101.
[48] Y. Guo, S. Yang, W. Fu, J. Qi, R. Li, Z. Wang, H. Xu, Adsorption of malachite green on micro- and mesoporous rice husk-based active carbon, Dyes Pigments 56 (2003) 219–229.
[49] M. Alkan, M. Doğan, Y. Turhan, Ö. Demirbaş, P. Turan, Adsorption kinetics and mechanism of maxilon blue 5G dye on sepiolite from aqueous solutions, Chem. Eng. J. 139 (2008) 213–223.
[50] S. Lagergren, Zur theorie der sogenannten adsorption geloster stoffe. Kungliga Svenska Vetenskapsakademiens, Handlingar. Band. 24 (4) (1898) 1–39.
[51] Y.S. Ho, G. McKay, The kinetics of sorption of basic dyes from aqueous solution by sphagnum moss peat, Can. J. Chem. Eng. 76 (4) (1998) 822–827.
[52] D. Kavitha, C. Namasivayam, Experimental and kinetic studies on methylene blue adsorption by coir pith carbon, Bioresour. Technol. 98 (1) (2007) 14–21.
[53] O. Hamdaoui, Batch study of liquid-phase adsorption of methylene blue using cedar sawdust and crushed brick, J. Hazard. Mater. B135 (2006) 264–273.
[54] M. Doğan, Y. Özdemir, M. Alkan, Adsorption kinetics and mechanism of cationic methyl violet and methylene blue dyes onto sepiolite, Dyes Pigments 75 (3) (2007) 701–713.
[55] A.P. Mathews, W.J. Weber, Effects of external mass transfer and inler-particle diffusion on adsorption, AIChE Symp. Ser. 73 (1976) 91–98.
[56] K.G. Bhattacharyya, A. Sharma, Kinetics and thermodynamics of Methylene Blue adsorption on Neem (*Azadirachta indica*) leaf powder, Dyes Pigments 65 (2005) 51–59.
[57] W.J. Weber, J.C. Morris, Kinetics of adsorption on carbon from solution, J. Sanit. Eng. Div. Am. Soc. Civ. Eng. 89 (1963) 31–60.
[58] Y.S. Ho, Removal of copper ions from aqueous solution by tree fern, Water Res. 37 (10) (2003) 2323–2330.
[59] K.V. Kumar, A. Kumaran, Removal of methylene blue by mango seed kernel powder, Biochem. Eng. J. 27 (2005) 83–93.
[60] M. Al-Ghouti, M.A.M. Khraisheh, M.N.M. Ahmad, S. Allen, Thermodynamic behaviour and the effect of temperature on the removal of dyes from aqueous solution using modified diatomite: a kinetic study, J. Colloid Interface Sci. 287 (2005) 6–13.
[61] W.J. Thomas, B. Crittenden, Adsorption Technology and Design, Reed Educational and Professional Publishing, Oxford, 1998, pp. 27, 32, 68.
[62] H. Nollet, M. Roels, P. Lutgen, P. Van der Meeren, W. Verstraete, Removal of PCBs from wastewater using fly ash, Chemosphere 53 (2003) 655–665.
[63] M. Sankar, G. Sekaran, S. Sadulla, T. Ramasami, Removal of diazo and triphenylmethane dyes from aqueous solutions through an adsorption process, J. Chem. Technol. Biotechnol. 74 (1999) 337–344.
[64] K.J. Laidler, J.M. Meiser, Physical Chemistry, Houghton Mifflin, New York, 1999, p. 852.
[65] T.S. Anirudhan, P.G. Radhakrishnan, Thermodynamics and kinetics of adsorption of Cu(II) from aqueous solutions onto a new cation exchanger derived from tamarind fruit shell, J. Chem. Thermodyn. 40 (2008) 702–709.